Proceedings of the 10th
World Congress on Intelligent Control and Automation
July 6-8, 2012, Beijing, China

Tracking Control for Nonholonomic Mobile Robots with Visual Servoing Feedback *

Baolei Wang and Chaoli Wang
School of Optical-Electrical and Computer Engineering
University of Shanghai for Science and Technology
Shanghai , China,200093
bolly1986518@163.com
clclwang@126.com

***Abstract* - This paper discusses a tracking control problem of nonholonomic mobile robots with visual servoing feedback. By comparing corresponding target points of an object from two different camera images, geometric relationships are exploited to derive a transformation that relates the actual position and orientation of the mobile robot to a reference position and orientation. This transformation is used to synthesize a rotation and translation error system from the current position and orientation to the fixed reference position and orientation. Lyapunov-based techniques are used to construct a robust controller to stabilize the error system with a constant, unmeasurable depth parameter. The contribution of this paper is that Lyapunov techniques are used to construct a robust controller that makes mobile robot position and orientation converge to the desired configuration despite the lack of an object model and the lack of depth information. Simulation results are provided to illustrate the performance of the controller**

***Index Terms* - Robust control, homography, Lyapunov techniques, visual servo.**

I. INTRODUCTION

Visual servo algorithms have been extensively developed in the robotics field over the last ten years [1]. Most visual servo control has been developed for serial-link robotic manipulators with the camera typically mounted on the end-effector [2]. Visual servo systems may be divided into two main classes [1, 3]: *Position-based visual servo* (PBVS) and *Image-base visual servo* (IBVS) [1]. However, each kind of approaches has its own problems[10,11].

Various approaches have been reported including estimation via partial pose estimation[3], adaptive control [4] and estimation of the image Jacobin using quasi-Newton techniques [5,6]. More recently, there has been considerable interest in hybrid control methods whereby translational and rotational control are treated separately[3,7]. Hybrid methods, however, share with the P BVS approach a difficulty to keep all image features within the camera's field of view. Contemporary work [8,9] aims to address these issues.

With the success of image extraction technology and advances in control theory, there are lots of literatures has focused on the use of monocular camera-based vision systems for navigating a mobile robot [12,13]. A significant issue with monocular camera-based vision systems is the lack of depth information. Various approaches have been proposed to discuss the problem[14,15,16].

Recently, mobile robot visual servo tracking controllers were proposed with one camera onboard[17,16,18]. The methods are not constrained to a planar application. However, these results cannot be applied to solve the mobile robot regulation problem due to restrictions on the mobile robot reference velocity (i.e., the reference linear velocity cannot converge to zero).

A monocular two-and-one-half-dimensional (2.5-D) visual servo control methodology was developed for unconstrained systems (e.g., robot manipulators) in a series of papers by Malis and Chaumette (e.g., [19,20],[21 — 23]). Specifically, the 2.5-D visual servo control method exploits a combination of reconstructed three-dimensional (3-D) task-space information and two-dimensional (2-D) image-space information.

Recently, Fang *et al.* [24] developed asymptotic regulation controller of the position/orientation of a mobile robot based on a homography visual servo that adaptively compensates for the unknown time-varying depth parameter for a monocular camera system mounted in the camera-in-hand. The contribution of this paper is that a new analytical approach has been developed using homography-based concepts to enable a mobile robot to be regulated to a desired position/orientation based on a desired image, despite the lack of depth measurements. However, the error convergence of the third coordinate component needs certain strict conditions.

In this paper, robust asymptotic stabilization of the position/orientation of a mobile robot is achieved by exploiting homography-based visual servo control strategies inspired by the work given in [20 ， 24] and [23]. By comparing the features of an object in the reference image to features of the object in the current image, image-based geometric relationships are exploited to construct a

* This work is partially supported by The Nature Science Foundation(60874002), Leading Academic Discipline Project of Shanghai Municipal Government(S30501), The Innovation Fund Project For Graduate Student of Shanghai(JWCXSL1102), Shanghai High Education Connotation Construction Project ("085 Project") of 2012.

978-1-4673-1398-8/12/$31.00 ©2012 IEEE

homography matrix despite the fact that a geometric model of the object is not known. Under the assumption of the unknown depth with a known positive lower limit, a robust controller is constructed to stabilize the error system. The contribution of this paper is that Lyapunov techniques are exploited to craft a robust controller that enables mobile robot position and orientation regulation with an unknown object model and unknown depth information.

II. Model

The objective of this paper is to stabilize the position/orientation of a mobile robot based on image-feedback of a fixed target. As illustrated in Fig. 1, the origin of the orthogonal coordinate system Γ attached to the camera is coincident with the center of mass of the mobile robot. As also illustrated in Fig. 1, the xy axis of Γ defines the mobile robot plane of motion where the x axis of Γ is aligned with the front of the mobile robot, and the y axis is parallel to the wheel axis. The z axis of Γis perpendicular to the mobile robot plane of motion and is located at the center of the wheel axis. The linear velocity of the mobile robot along the axis x is denoted by $v_c(t)$, and the angular velocity $\omega_c(t)$ is about the x axis. In addition to Γ, another fixed orthogonal coordinate system, denoted by Γ^*, is defined to represent the desired fixed position and orientation of the camera relative to a target. Hence, the goal is to develop a controller that will regulate the position and orientation of Γ to Γ^*.

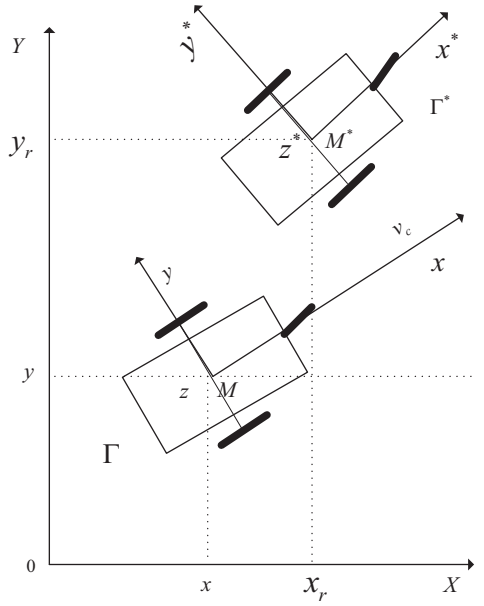

Fig. 1. Nonholonomic mobile robot coordinate systems

In this paper, the target is assumed to be distinguished by three points $O_i,\ i=1,2,3$, that compose a plane, denoted by π . The Euclidean position of point expressed in the coordinate frames Γ and Γ^* is denoted by $\bar{m}_i(t),\ \bar{m}_i^* \in \mathbb{R}$, respectively, and is defined as follows (see Fig. 2):

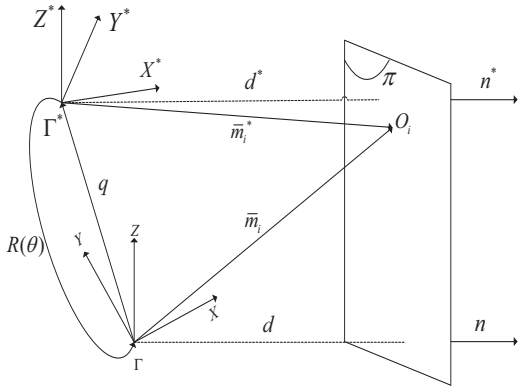

Fig. 2. Geometric relationship of the mobile robot system.

$$\begin{cases} \bar{m}_i(t) = \begin{bmatrix} x_i(t) & y_i(t) & z_i(t) \end{bmatrix}^T, \\ \bar{m}_i^* = \begin{bmatrix} x_i^* & y_i^* & z_i^* \end{bmatrix}^T \end{cases} \tag{1}$$

Since the 3-D Euclidean position of the point O_i is observed from the 2-D image-space of the camera, normalized position vectors are defined as follows:

$$\begin{aligned} m_i(t) &= \begin{bmatrix} 1 & m_{iy}(t) & m_{iz}(t) \end{bmatrix}^T = \frac{\bar{m}_i(t)}{x_i(t)} \\ &= \begin{bmatrix} 1 & \dfrac{y_i(t)}{x_i(t)} & \dfrac{z_i(t)}{x_i(t)} \end{bmatrix}^T \\ m_i^* &= \begin{bmatrix} 1 & m_{iy}^* & m_{iz}^* \end{bmatrix}^T = \frac{\bar{m}_i^*}{x_i^*} \\ &= \begin{bmatrix} 1 & \dfrac{y_i^*}{x_i(t)} & \dfrac{z_i^*}{x_i(t)} \end{bmatrix}^T \end{aligned} \tag{2}$$

where the standard assumption is made that x_i^* and $x_i(t)$ are positive [27] (i.e., the target is always in front of the camera). In addition to the normalized Euclidean position, each point has an image-space representation, denoted by $p_i(t),\ p_i^* \in \mathbb{R}$

$$\begin{cases} p_i(t) = \begin{bmatrix} 1 & u_i(t) & v_i(t) \end{bmatrix}^T, \\ p_i^* = \begin{bmatrix} 1 & u_i^* & v_i^* \end{bmatrix}^T \end{cases} \tag{3}$$

where $v_i(t),\ u_i(t) \in \mathbb{R}$ denote the pixel coordinates of the point O_i . The image-space coordinates given in (3) are related to the normalized coordinates given in (2) by the following invertible transformation (i.e., the pinhole camera model):

$$m_i = A^{-1} p_i,\ m_i^* = A^{-1} p_i^* \quad (4)$$

where $A \in \mathbb{R}$ denotes a constant, invertible matrix composed of the intrinsic camera calibration parameters [27]. Since the camera is assumed to be calibrated (i.e., the matrix A is assumed to be known), and can be calculated using (4) from the known camera pixel-space vectors $p_i(t),\ p_i^*$. The main idea behind the current visual servoing strategy is to extract 2-D information from the environment using the camera image and then determine 3-D information through a Euclidean reconstruction. The Euclidean reconstruction is performed by exploiting the geometry between the features of the target (image points) in the camera's current image to the desired image. Based on the geometric relationships, a homography matrix can be calculated to relate the projected 3-D position to the image-space position of the target[23]. For example, the geometric relationships between Γ and Γ^* can be determined from Fig. 2. In Fig. 2, $\theta(t) \in \mathbb{R}$ is the angle between the axes x^* and x, the unit vectors, $n^*, n(t) \in \mathbb{R}$ are normal to the plane π expressed in Γ and Γ^*, respectively, and $d^*, d(t) \in \mathbb{R}$, are the unknown, positive distances from the origin of Γ^* and Γ to the plane π along n^* and $n(t)$, respectively. Based on Fig. 2, the following relationship can be determined:

$$\bar{m}_i = R\bar{m}_i^* + q(t) \quad (5)$$

In (5), $R(t) \in SO(3)$ denotes the following rotation matrix from Γ^* to Γ:

$$R = \begin{bmatrix} \cos(\theta) & -\sin(\theta) & 0 \\ \sin(\theta) & \cos(\theta) & 0 \\ 0 & 0 & 1 \end{bmatrix} \quad (6)$$

and $q(t) \in \mathbb{R}$ is the translation vector from Γ to Γ^* given by

$$q(t) = \begin{bmatrix} q_x(t) & q_y(t) & 0 \end{bmatrix}^T \quad (7)$$

Since d^* is the projection of $\bar{m}_i^*$ along n^*, the following relationship can be determined:

$$d^* = \left(n^*\right)^T \bar{m}_i^* \quad (8)$$

Using (8), the expression given in (5) can be rewritten as

$$\bar{m}_i = H\bar{m}_i^* \quad (9)$$

where the Euclidean homography $H(t) \in \mathbb{R}$ is defined as follows:

$$H = R + \frac{q}{d^*}\left(n^*\right)^T \quad (10)$$

By using (6), (7), and (10), the Euclidean homography can be rewritten as follows:

$$H = \left[H_{jk}\right] = \begin{bmatrix} \cos(\theta) + \frac{q_x n_x^*}{d^*} & -\sin(\theta) + \frac{q_x n_y^*}{d^*} & \frac{q_x n_z^*}{d^*} \\ \sin(\theta) + \frac{q_y n_x^*}{d^*} & \cos(\theta) + \frac{q_y n_y^*}{d^*} & \frac{q_y n_z^*}{d^*} \\ 0 & 0 & 1 \end{bmatrix} \quad (11)$$

where $n^* = \begin{bmatrix} n_x^* & n_y^* & n_z^* \end{bmatrix}^T$. By examining the terms in (11), it is clear that $H(t)$ contains signals that are not directly obtained from the vision system (e.g., $\theta(t)$, $q(t)$ and d^* are not directly available from the camera image). However, the six unknown elements of $H_{jk}(t)$, $\forall j = 1, 2$, $k = 1, 2, 3$, can be determined indirectly from the image coordinates by solving a set of linear equations. Specifically, by using the definition given in (2), the expression given in (9) can be rewritten as follows:

$$m_i = \left(\frac{x_i^*}{x_i}\right) H m_i^* \quad (12)$$

$$\gamma i$$

where $r_i(t) \in \mathbb{R}$ denotes a depth ratio. By expanding (12), the following expressions can be obtained:

$$1 = \gamma_i \left(H_{11} + H_{12} m_{iy}^* + H_{13} m_{iz}^*\right) \quad (13)$$

$$m_{iy} = \gamma_i \left(H_{21} + H_{22} m_{iy}^* + H_{23} m_{iz}^*\right) \quad (14)$$

$$m_{iz} = \gamma_i m_{iz}^* \quad (15)$$

Given that (13)–(15) will be generated for each of the three target points, a total of nine independent equations will result. Given the nine independent equations, the nine unknown parameters(i.e., $H_{jk}(t)$, $\forall j = 1, 2$, $k = 1, 2, 3$ and $r_i(t)$, $\forall i = 1, 2, 3$) can be determined. Based on the fact that the elements of the homography matrix and the depth ratio can be determined, various techniques can now be applied [16], [37], [38] to decompose $H(t)$ to obtain $R(t)$, $\gamma_i(t)$, and $q(t)n^*/d^*$; hence, $\theta(t)$ and $\gamma_i(t)$ can be calculated and used in the subsequent control development. To compute $\theta(t)$ from $R(t)$ the following expression can be utilized [31]:

$$\theta = \cos^{-1}\left(\frac{1}{2}\left(tr\left(R\right)\right) - 1\right)$$

where $0 \le \theta(t) \le \pi$.

III. PROBLEM FORMULATION

The control objective is to ensure that the coordinate frame attached to the mobile robot is regulated to the fixed

coordinate frame Γ^*. This objective is naturally defined in terms of the Euclidean position/orientation of the mobile robot. Specifically, the translation error between Γ and Γ^*, denoted by $e_t(t) \in \mathbb{R}$, can be written for any target point $O_i,\ i=1,2,3$, as follows:

$$e_t = \begin{bmatrix} e_{tx} \\ e_{ty} \end{bmatrix} = \begin{bmatrix} q_x \\ q_y \end{bmatrix} = \begin{bmatrix} x_i \\ y_i \end{bmatrix} - \begin{bmatrix} \cos(\theta) & -\sin(\theta) \\ \sin(\theta) & \cos(\theta) \end{bmatrix} \begin{bmatrix} x_i^* \\ y_i^* \end{bmatrix} \quad (16)$$

where (5)–(7) have been utilized. The orientation error between Γ and Γ^*, denoted by $e_o(t) \in \mathbb{R}$, can be written as follows:

$$e_o(t) = \theta(t) \quad (17)$$

where was defined in (6). Based on the definitions of (16) and (17), the control objective is to regulate $e_t(t)$ and $e_o(t)$ to zero. The open-loop error system for $e_o(t)$ and $e_t(t)$ can be determined by taking the time derivative of (16) and (17) and then utilizing the fact that the time derivative of the Euclidean position given in (1) can be determined as follows [11], [27]:

$$m_i' = -v - \omega \times \bar{m}_i \quad (18)$$

where $v(t)$, $\omega(t) \in \mathbb{R}$ denote the linear and angular velocity of the mobile robot expressed in Γ as

$$\begin{aligned} v(t) &= \begin{bmatrix} v_c(t) & 0 & 0 \end{bmatrix}^T \\ \omega(t) &= \begin{bmatrix} 0 & 0 & \omega_c(t) \end{bmatrix}^T = \begin{bmatrix} 0 & 0 & -\theta'(t) \end{bmatrix}^T \end{aligned} \quad (19)$$

respectively. From the expression given in (1), (18), and (19), the Euclidean mobile robot velocity can be written in terms of the linear and angular velocity as follows:

$$\begin{aligned} x_i' &= -v_c + y_i \omega_c \\ y_i' &= -x_i \omega_c \end{aligned} \quad (20)$$

After utilizing (16), (19), and (20) the following open-loop error system can be obtained:

$$\begin{aligned} e_{tx}' &= -v_c + \omega_c e_{ty} \\ e_{ty}' &= -\omega_c e_{tx} \\ e_o' &= -\omega_c \end{aligned} \quad (21)$$

where (16) was utilized.

Ⅳ. Controller Design

The structure of the resulting open-loop error system developed in (21) has been extensively examined in mobile robot control literature. However, unlike the typical mobile robot control problem, the Euclidean translation error signals $e_{tx}(t)$ and $e_{ty}(t)$ are unmeasurable, and hence, new analytical development

is required to overcome this conundrum. To address this issue, an adaptive controller is developed in this section that actively compensates for the unknown depth information through a gradient-based adaptive update law.

To facilitate the subsequent control design,2 a composite translation and rotation error signal, denoted by $r(t) \in \mathbb{R}$, is defined as follows:

$$r = \begin{bmatrix} r_1(t) & r_2(t) & r_3(t) \end{bmatrix} = \begin{bmatrix} -e_o & -\frac{e_{tx}}{x_i^*} & \frac{e_{ty}}{x_i^*} \end{bmatrix} \quad (22)$$

By utilizing the relationship introduced in (16), the following expressions can be developed for $r_2(t)$ and $r_3(t)$:

$$r_2 = -\left[\frac{1}{\gamma i} - \cos(\theta) + m_{iy}^* \sin(\theta) \right] \quad (23)$$

$$r_3 = \left[\frac{1}{\gamma i} m_{iy} - \sin(\theta) - m_{iy}^* \cos(\theta) \right] \quad (24)$$

From the expressions given in (22)–(24), it is clear that $r_1(t)$, $r_2(t)$ and $r_3(t)$ can be computed from (13)–(15) and the decomposition of the homography matrix. After taking the time derivative of (22) and utilizing (21), the resulting simplified open-loop dynamics for $r(t)$ can be determined as follows:

$$\begin{aligned} r_1' &= \omega_c \\ \alpha r_2' &= v_c - \alpha \omega_c r_3 \\ r_3' &= \omega_c r_2 \end{aligned} \quad (25)$$

where (22) has been utilized, and $\alpha \in \mathbb{R}$ denotes the following positive constant:

$$\alpha = x_i^* \quad (26)$$

Introducing new coordinates and control input as following:

$$\begin{cases} x_1 = r_1 \\ x_2 = r_2 \\ x_3 = r_3 \end{cases}, \quad v_c = u_2,\ \omega_c = u_1$$

Using (25) yields

$$\begin{cases} x_1' = u_1 \\ x_2' = \dfrac{1}{\alpha} u_2 - u_1 x_3 \\ x_3' = u_1 x_2 \end{cases} \quad (27)$$

where $\alpha = x_i^*$ is unknown. Let $\dfrac{1}{\alpha} = r$. Then it has

$$\begin{cases} x_1' = u_1, \\ x_2' = r u_2 - u_1 x_3, \\ x_3' = u_1 x_2 \end{cases} \quad (28)$$

In order to describe the main theorems easily, the following lemma is needed(easily seen literature).

Lemma：Consider the linear time-varying system below

$$x' = (A_1 + A_2(t))x \quad (29)$$

If A_1 is a Hurwitz matrix，and $A_2(t)$ satisfies the conditions that the limitation of $A_2(t)$ is 0 when t is infinity and the integration of $A_2(t)$'s 2-norm from zero to infinity is smaller than infinity, the system(29) is exponentially asymptotical stable in the sense of global.

Theorem 1: Suppose $r_1(0) \neq 0$ and $r \geq r_0$,where r_0 is a known positive number.Choose k_1, k_2 and k such that

$$\begin{cases} k > 0 \\ k_1 < -\dfrac{k}{r_0} \\ k_2 > -k_1 k \end{cases} \qquad (30)$$

Then

(1) $A_1 = \begin{pmatrix} rk_1 & rk_2 \\ -k & k \end{pmatrix}$ is a Hurwitz matrix.

(2) the system(28) can be stabilized to zero by the controller described as following

$$\begin{cases} u_1 = -kx_1 \\ u_2 = k_1 x_2 + k_2 \dfrac{x_3}{x_1} \end{cases} \qquad (31)$$

In theorem 1, there is an assumption $r_1(0) \neq 0$. It is inconvenient for practical use. In fact, it can be cancelled.

Theorem 2: Suppose $r \geq r_0$, where r_0 is a known positive number. Choose k_0, β, k_1, k_2 and k such that

$$\begin{cases} k_1 \leq -\dfrac{\beta}{r_0}, k_0 \neq 0 \\ k > \beta > 0 \\ -k_2 < k_1(k-\beta) \end{cases}$$

The controller described as following

$$\begin{cases} u_1 = -kx_1 + k_0 e^{-\beta t} \\ u_2 = k_1 x_2 + k_2 \dfrac{x_3}{k_0 e^{-\beta t}} \end{cases} \qquad (32)$$

can make the states of system (28) converge to zero.

Ⅴ. Simulation

The simulation will be done based on the system (28).

5.1 $r_1(0) \neq 0$

Take the initial value $(\frac{2\pi}{3}, -3, 5)$ and the controller is chosen like (31). Choose r_0=0.2m , r =0.4m , $k_1 = -32$, $k_2 = 200$, $k = 6$. The responses of states of the system with respect to time are shown in Figure 3.

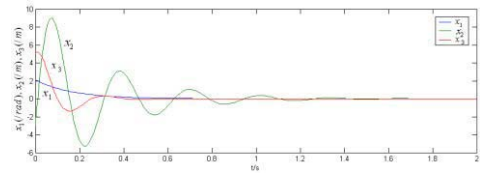

Figure 3 The response of the states of the system (28) with respect to time

5.2 $r_1(0)$ is given arbitrarily

Take the initial value $(\frac{2\pi}{3}, 3, 5)$. The controller is chosen as (39). Choose β=1 , k_0=1 , r_0=0.2m , r =0.4m , $k_1 = -6$, $k_2 = 30$, $k = 3$. The simulation is implemented based on system (28). The results are shown in Figure 4.

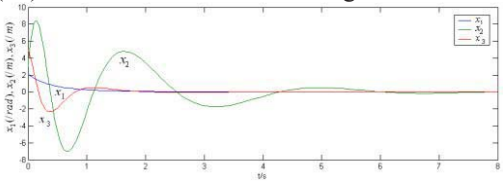

Figure 4 The response of the states of the system (28) with respect to time

Remark 1. By comparing Figure 3 and Figure 4, it is seen that the time to spend for converging to zero by using the controller in theorem 2 is much than that in theorem 1. This is because the controller in theorem 2 is added an exponential term, which can be understood as a kind of disturbance. This disturbance can delay the convergence.

Ⅵ. Conclusion

In this paper, asymptotic stabilization of the position/orientation of a WMR is achieved with a monocular vision system. By comparing the features of an object from an initial snapshot to features of the object in the current image, geometric relationships are exploited to determine a Euclidean homography that relates the image-space feedback to the actual Euclidean position/orientation of the camera (and hence the WMR) in a local coordinate system. By decomposing the homography into separate translation and rotation components, we were able to exploit reconstructed 3D task-space information to construct the kinematic controller. The control design is based on kniematic model of WMR. The similar idea can be extended to the dynamic model of WMR. Future efforts will also target real-time experimental demonstration of the proposed controllers.

ACKNOWLEDGE

This paper is supported by National Nature Science Foundation(60874002), Shanghai Leading Academic Discipline Project(S30501), The Innovation Fund Project For Graduate Student of Shanghai (JWCXSL1102), Shanghai High Education Connotation Construction Project ("085 Project") of 2012.

REFERENCES

[1] B. Espiau, F. Chaumette, and P. Rives. A new approach to visual servoing in robotics. *IEEE Transactions on Robotics and Automation,* 8(3):313-326, 1992.

[2] S. Hutchinson, G. Hager, and P. Cork. A tutorial on visual servo control. *IEEE Transactions on Robotics and Automation,* 12(5):651-670, 1996.

[3] E. Malls, F. Chaumette, and S. Boudet. 2-1/2-D visual servoing. *IEEE Transactions on Robotics and Automation,* 15(2):238-250, April 1999.

[4] N. Papanikolopoulos, P. K. Khosla, and T. Kanade. Adaptive robot visual tracking. In *Proceedings of the American Control Conference,* pages 962-967, 1991.

[5] K. Hosada and M. Asada. Versatile visual servoing without knowledge of true jacobian. In *Proceedings of the IEEE/RSJ International Conference on Intelligent Robots and Systems,* pages 186-193, Munich, Germany, 1994.

[6] J.A. Piepmeier. *A dynamic quasi-newton method for model independent visual servoing.* P hd, Georgia Institute of Technology, Atlanta, USA, July 1999.

[7] K. Deguchi. Optimal motion control for imagebased visual servoing by decoupling translation and rotation. In *Proceedings of the International Conference on Intelligent Robots and Systems,* pages 705-711, 1998.

[8] G. Morel, T. Liebezeit, J. Szewczyk, S. Boudet, and J. Pot. *Explicit incoporation of 2D constraints in vision*
based control of robot manipulators, volume 250 of *Lecture Notes in Control and Information Sciences,* pages 99-108. Springer-Verlag, New York, USA, 1999. Edited by P. Corke and J. Trevelyan.

[9] P.I. Corke and S. A. Hutchinson. A new partitioned approach to image-based visual servo control. In
Proceedings of the International Symposium on Robotics, Montreal, Canada, May 2000.

[10] A. Castano and S. Hutchinson. Visual compliance: Task directed visual servo control. *IEEE trasnactions on Robotics and Automation,* 10(3):334-341, June 1993.

[11] F. Chaumette. Potential problems of stability and convergence in image-based and position-based visual servoing. In *The Confluence of Vision and Control,* LNCIS, No. 237 pp. 66-78, 1998.

[12] M. Hebert, "3-D vision for outdoor navigation by an autonomous vehicle," presented at the *Image Understanding Workshop*, Cambridge.

[13] A. M.Waxman *et al.*, "A visual navigation system for autonomous land vehicles," *IEEE J. Robot. Autom.*, vol. RA-3, no. 2, pp. 124–141, Apr. 1987.

[14] B. H. Kim *et al.*, "Localization of a mobile robot using images of a moving target," in *Proc. IEEE Int. Conf. Robotics Automation*, 2001, pp. 253–258.

[15] A. K. Das *et al.*, "Real-time vision-based control of a nonholonomic mobile robot," in *Proc. IEEE Int. Conf. Robotics and Automation*, 2001, pp. 1714–1719.

[16] W. E. Dixon, D. M. Dawson, E. Zergeroglu, and A. Behal, "Adaptive tracking control of a wheeled mobile robot via an uncalibrated camera system," in *Proc. IEEE American Control Conf.*, Chicago, IL, Jun. 2000, pp. 1493–1497.

[17] J. Chen,W. E. Dixon, D. M. Dawson, and M. McIntyre, "Homographybased visual servo tracking control of a wheeled mobile robot", *IEEE Trans. Robot.*, to be published.

[18] H. Y. Wang, S. Itani, T. Fukao, and N. Adachi, "Image-based visual adaptive tracking control of nonholonomic mobile robots," in *Proc. IEEE/RJS Int. Conf. Intelligent Robots and Systems*, 2001, pp. 1–6.

[19] F. Chaumette and E. Malis, "2 1/2 D visual servoing: A possible solution to improve image-based and position-based visual servoings," in *Proc. IEEE Int. Conf. Robotics and Automation*, 2000, pp. 630–635.

[20] F. Chaumette, E. Malis, and S. Boudet, "2D 1/2 visual servoing with respect to a planar object," in *Proc. Workshop on New Trends in Image-Based Robot Servoing*, 1997, pp. 45–52.

[21] E. Malis, "Contributions à la modélization et à la commande en asservissement visuel," Ph.D. dissertation, Univ. Rennes I, IRISA, Paris, France, Nov. 1998.

[22] E. Malis and F. Chaumette, "2 1/2 D visual servoing with respect to unknown objects through a new estimation scheme of camera displacement," *Int. J. Comput. Vis.*, vol. 37, no. 1, pp. 79–97, Jun. 2000.

[23] E. Malis, F. Chaumette, and S. Bodet, "2 1/2 D visual servoing," *IEEE Trans. Robot. Autom.*, vol. 15, no. 2, pp. 238–250, Apr. 1999.

[24] Yongchun Fang*, et al.*, IEEE TRANSACTIONS ON SYSTEMS, MAN, AND CYBERNETICS—PART B: CYBERNETICS, VOL. 35, NO. 5, PP. 1041-1050, OCTOBER 2005.